2HDM CONFRONTING LHC DATA

P.M. FERREIRA

Instituto Superior de Engenharia de Lisboa - ISEL, 1959-007 Lisboa, Portugal

Centro de Física Teórica e Computacional, Faculdade de Ciências, Universidade de Lisboa, Av. Prof. Gama Pinto 2, 1649-003 Lisboa, Portugal

RUI SANTOS

Instituto Superior de Engenharia de Lisboa - ISEL, 1959-007 Lisboa, Portugal

Centro de Física Teórica e Computacional, Faculdade de Ciências, Universidade de Lisboa, Av. Prof. Gama Pinto 2, 1649-003 Lisboa, Portugal

MARC SHER

High Energy Theory Group, College of William and Mary, Williamsburg, Virginia 23187, U.S.A.

JOÃO P. SILVA

Instituto Superior de Engenharia de Lisboa, 1959-007 Lisboa, Portugal

Centro de Física Teórica de Partículas (CFTP), Instituto Superior Técnico, Universidade Técnica de Lisboa, 1049-001 Lisboa, Portugal

Almost all data collected at the LHC during the 7 and 8 TeV runs has now been analysed by the ATLAS and CMS collaborations. Its consistency with the Standard Model (SM) predictions has cornered the CP-conserving two-Higgs doublet model (2HDM) into the SM limit, $\sin(\beta - \alpha) = 1$. However, there are still allowed regions of the 2HDM parameter space away from this limit. In this work we discuss how the 2HDM is performing in view of the LHC data together with the remaining available experimental and theoretical constraints.

1 Introduction

The discovery of a neutral Higgs boson [1] at CERN's Large Hadron Collider (LHC) has now been confirmed. Hence, all extensions of the Standard Model (SM) have to abide to the existence of a Higgs boson with SM like properties and with a mass of around 125 GeV. The two-Higgs doublet model (2HDM) is one of the simplest extension of the SM. It is built with the addition of a second complex scalar doublet to the SM field content. Consequently, one obtains a richer particle spectrum with one charged and three neutral scalars. All neutral scalars could in principle be the scalar discovered at the LHC [2]. However, a pure pseudo-scalar state with a 125 GeV mass has now been experimentally ruled out [3]. In the next section we present the 2HDM model and in the following sections we discuss how well the most common CP-conserving 2HDM can accommodate the LHC data.

2 The Model

The addition of a second complex scalar doublet to the SM's Yukawa Lagrangian gives rise to the appearance of scalar exchange flavour changing neutral currents (FCNCs) which are known to be strongly constrained by experiment. Avoiding those dangerous FCNCs can be accomplished by simply imposing a Z_2 symmetry on the scalar doublets, $\Phi_1 \to \Phi_1$, $\Phi_2 \to -\Phi_2$, and a corresponding symmetry to the fermion fields. This leads to the well known four Yukawa model types I, II, Y (III, Flipped) and X (IV, Lepton Specific) [4]. The scalar potential in a softly broken Z_2 symmetric 2HDM can be written as

$$\begin{aligned} V(\Phi_1,\Phi_2) &= m_1^2\Phi_1^\dagger\Phi_1 + m_2^2\Phi_2^\dagger\Phi_2 + (m_{12}^2\Phi_1^\dagger\Phi_2 + \text{h.c.}) + \frac{1}{2}\lambda_1(\Phi_1^\dagger\Phi_1)^2 + \frac{1}{2}\lambda_2(\Phi_2^\dagger\Phi_2)^2 \\ &\quad +\lambda_3(\Phi_1^\dagger\Phi_1)(\Phi_2^\dagger\Phi_2) + \lambda_4(\Phi_1^\dagger\Phi_2)(\Phi_2^\dagger\Phi_1) + \frac{1}{2}\lambda_5[(\Phi_1^\dagger\Phi_2)^2 + \text{h.c.}]\ , \end{aligned} \tag{1}$$

where Φ_i, $i = 1, 2$ are complex SU(2) doublets. All parameters except for m_{12}^2 and λ_5 are real as a consequence of the hermiticity of the potential. We will focus on the CP-conserving potential where m_{12}^2, λ_5 and the VEVs are all real. In this model the three CP-eigenstates are usually denoted by h and H (CP-even) and A (CP-odd). As shown in [5], once a CP-conserving vacuum configuration is chosen, all charge breaking stationary points are saddle points with higher energy. Hence, the 2HDM is stable at tree-level against charge breaking and once a non-charge breaking vacuum is chosen the model has two charged Higgs bosons that complete the 2HDM particle spectrum. We choose as free parameters of the model, the four masses, the rotation angle in the CP-even sector, α, the ratio of the vacuum expectation values, $\tan\beta = v_2/v_1$, and the soft breaking parameter redefined as $M^2 = m_{12}^2/(\sin\beta\cos\beta)$ (see [6] for a review of the model). The remaining theoretical and experimental constraints used in this work were recently discussed in [7].

3 Results and discussion

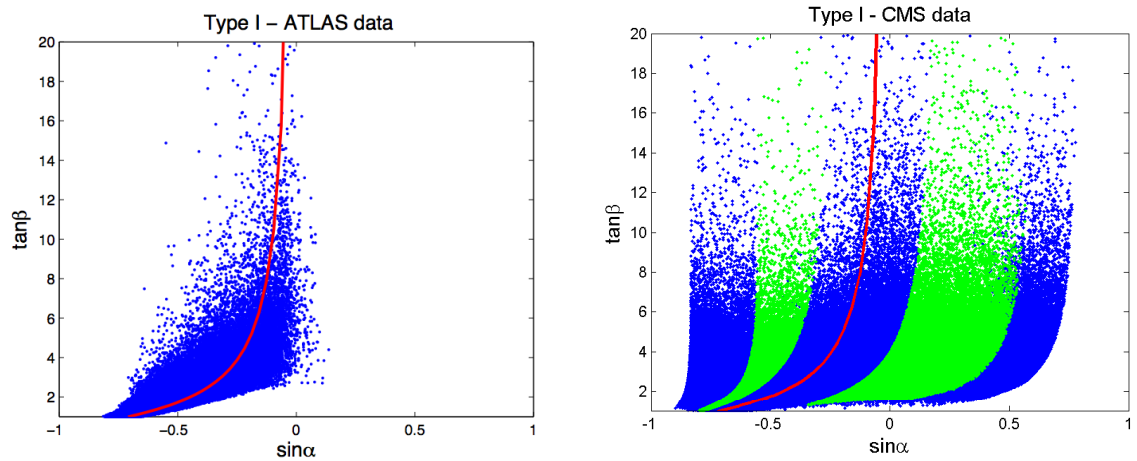

Figure 1: Points in the ($\sin\alpha$, $\tan\beta$) plane that passed all the constraints in model type I using the ATLAS data analysis (left) and using the CMS data analysis (right) at 1σ in green (light grey) and 2σ in blue (dark grey). Also shown is the line for the SM limit $\sin(\beta-\alpha) = 1$.

We randomly generate points in the model's parameter space such that $m_h = 125$ GeV, 90 GeV $\leq m_A \leq 900$ GeV, $m_h < m_H \leq 900$ GeV, $1 \leq \tan\beta \leq 40$, $-(900)^2$ GeV$^2 \leq m_{12}^2 \leq 900^2$ GeV^2 and $-\pi/2 \leq \alpha \leq \pi/2$. In order to respect the flavour constraints we take 90 GeV $\leq m_{H^\pm} \leq 900$ GeV for type I while for type II the allowed range is 360 GeV $\leq m_{H^\pm} \leq 900$ GeV. We define the quantities R_f as the ratio of the number of events predicted in the 2HDM

to that obtained in the SM for a given final state f.

$$R_f = \frac{\sigma(pp \to h)_{\rm 2HDM}\ {\rm BR}(h \to f)_{\rm 2HDM}}{\sigma(pp \to h_{\rm SM})\ {\rm BR}(h_{\rm SM} \to f)}, \tag{2}$$

where h is the lightest CP-even Higgs (125 GeV), σ is the Higgs production cross section, BR the branching ratio, and $h_{\rm SM}$ is the SM Higgs boson. In our analysis, we include all Higgs production mechanisms, namely, gluon-gluon fusion using HIGLU at NLO [8], vector boson fusion (VBF) [9], Higgs production in association with either W, Z or $t\bar{t}$ [9], and $b\bar{b}$ fusion [10]. A number of similar studies where LHC data was used to constrain the 2HDM were presented in [11].

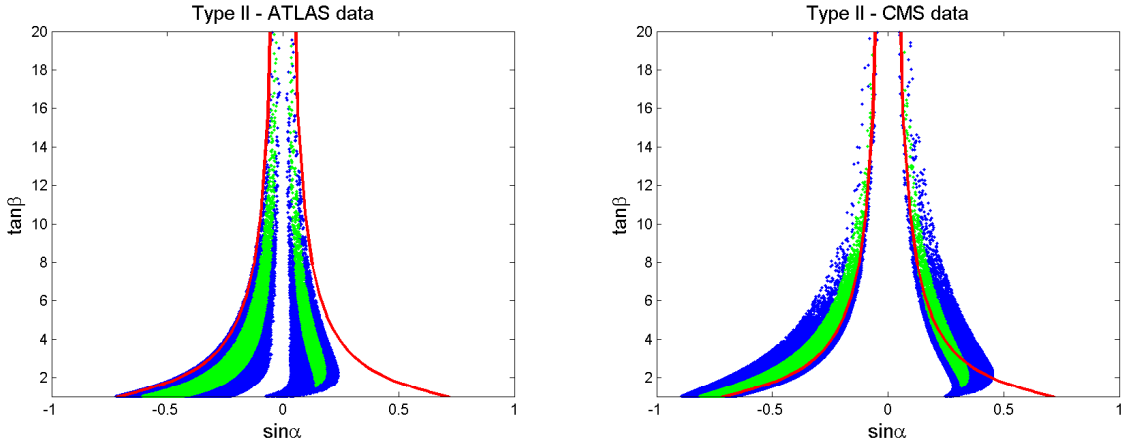

Figure 2: Points in the ($\sin\alpha$, $\tan\beta$) plane that passed all the constraints in model type II using the ATLAS data analysis (left) and using the CMS data analysis (right) at 1σ in green (light grey) and 2σ in blue (dark grey). Also shown are the lines for the SM limit $\sin(\beta-\alpha)=1$ (negative $\sin\alpha$) and for the limit $\sin(\beta+\alpha)=1$.

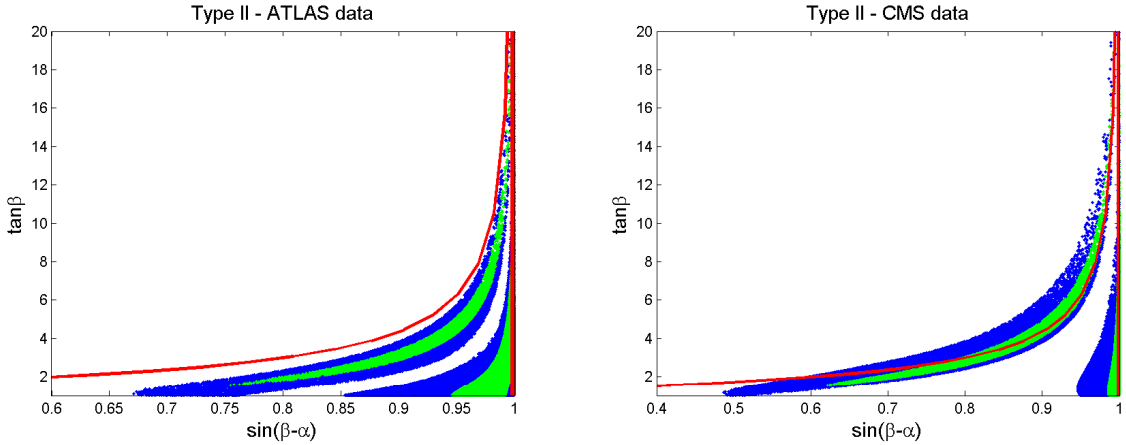

Figure 3: Points in the ($\sin(\beta-\alpha)$, $\tan\beta$) plane that passed all the constraints in model type II using the ATLAS data analysis (left) and using the CMS data analysis (right) at 1σ in green (light grey) and 2σ in blue (dark grey). Also shown are the lines for the SM limit $\sin(\beta-\alpha)=1$ and for the limit $\sin(\beta+\alpha)=1$.

In figure 1 we present the results for the type I model in the ($\sin\alpha$, $\tan\beta$) plane using the ATLAS data [12] (left) and the CMS data [13] (right). The differences between the two plots are easy to understand. The ATLAS data analysis forces R_{ZZ} to be large but as we have previously shown [7] R_{ZZ} can never be above one in type I. Consequently, no points survive at 1σ. With the CMS data analysis plenty of 1σ points survive because all R_{VV} are below one. The 1σ region is slightly away from the SM limit because the central values of R_{VV} are below one. Further, we see in both plots a large dispersion of values around the SM limit. The reason is that $R_{VV} \approx \sin^2(\beta-\alpha)$ in the limit where $BR(h \to b\bar{b}) \approx 1$ and this function is very sensitive from deviations from 1.

In figure 2 we now show similar plots for the type II model. In type II, R_{VV} is not a sensitive quantity [7]. Therefore both the 1σ and the 2σ points are very close to the two limiting lines. The difference between the two plots is that the points tend to concentrate below the limiting lines for ATLAS and above the same lines for CMS. This is of course a consequence of the central values of the ATLAS R_{VV} being above the SM while the CMS ones are below the SM expectation. Finally we present in figure 3 plots similar to the ones in figure 2 but now in the ($\sin(\beta-\alpha)$, $\tan\beta$) plane. Again we see the same trend with the allowed points on opposite sides of the limiting lines, $\sin(\beta-\alpha)=1$ and $\sin(\beta+\alpha)=1$. We should point out that remarkably (even being very conservative), we can already say that values of $\sin(\beta-\alpha)$ below 0.5 are excluded at 2σ. Even more interesting is that for values of $\sin(\beta-\alpha)$ below say 0.8 $\tan\beta$ has to be below 4. Hence, in type II large values of $\tan\beta$ are only allowed close to the SM limit.

Acknowledgments

The works of P.M.F. and R.S. are supported in part by the Portuguese *Fundação para a Ciência e a Tecnologia* (FCT) under contract PTDC/FIS/117951/2010, by FP7 Reintegration Grant, number PERG08-GA-2010-277025, and by PEst-OE/FIS/UI0618/2011. The work of J.P.S. is funded by FCT through the projects CERN/FP/109305/2009 and U777-Plurianual, and by the EU RTN project Marie Curie: PITN-GA-2009-237920. The work of MS is supported by the NSF under Grant No. PHY-1068008.

References

1. G. Aad *et al.* [ATLAS Collaboration], Phys. Lett. B **716**, 1 (2012); S. Chatrchyan *et al.* [CMS Collaboration], Phys. Lett. B **716**, 30 (2012).
2. P. M. Ferreira, R. Santos, M. Sher, J. P. Silva, Phys. Rev. D **85**, 077703 (2012); P. M. Ferreira, R. Santos, M. Sher, J. P. Silva, Phys. Rev. D **85**, 035020 (2012); G. Burdman, C. E. F. Haluch, R. D. Matheus, Phys. Rev. D **85**, 095016 (2012).
3. The ATLAS collaboration, ATLAS-CONF-2013-013; CMS-PAS-HIG-13-002.
4. V. D. Barger, J. L. Hewett and R. J. N. Phillips, Phys. Rev. D **41** (1990) 3421; M. Aoki, S. Kanemura, K. Tsumura and K. Yagyu, Phys. Rev. D **80** (2009) 015017.
5. P. M. Ferreira, R. Santos and A. Barroso, Phys. Lett. B **603** (2004) 219 [Erratum-ibid. B **629** (2005) 114]; A. Barroso, P. M. Ferreira, R. Santos, Phys. Lett. B **632**, 684 (2006); M. Maniatis, A. von Manteuffel, O. Nachtmann, F. Nagel, Eur. Phys. J. C **48**, 805 (2006); I. P. Ivanov, Phys. Rev. D **75**, 035001 (2007) [Erratum-ibid. D **76**, 039902 (2007)]; I. P. Ivanov, Phys. Rev. D **77**, 015017 (2008).
6. G. C. Branco, P. M. Ferreira, L. Lavoura, M. N. Rebelo, M. Sher and J. P. Silva, Phys. Rept. **516**, 1 (2012).
7. A. Barroso, P. M. Ferreira, R. Santos, M. Sher and J. P. Silva, arXiv:1304.5225 [hep-ph].
8. M. Spira, arXiv:hep-ph/9510347.
9. https://twiki.cern.ch/twiki/bin/view/LHCPhysics/CrossSectionsFigures #Higgs_production_cross_sections
10. R.V. Harlander and W.B. Kilgore, Phys. Rev. D **68**, 013001 (2003).
11. C. -Y. Chen and S. Dawson, Phys. Rev. D **87**, 055016 (2013) B. Coleppa, F. Kling and S. Su, arXiv:1305.0002 [hep-ph]; C. -W. Chiang and K. Yagyu, arXiv:1303.0168 [hep-ph]; M. Krawczyk, D. Sokolowska and B. Swiezewska, arXiv:1303.7102 [hep-ph]; A. Celis, V. Ilisie and A. Pich, arXiv:1302.4022 [hep-ph]; B. Grinstein and P. Uttayarat, arXiv:1304.0028 [hep-ph]; A. Arhrib, C. -W. Chiang, D. K. Ghosh and R. Santos, Phys. Rev. D **85**, 115003 (2012); [ATLAS Collaboration], ATLAS-CONF-2013-027.
12. The ATLAS collaboration, ATLAS-CONF-2013-012, ATLAS-CONF-2013-030, ATLAS-CONF-2013-034.
13. The CMS collaboration, CMS notes CMS-PAS-HIG-13-001, CMS-PAS-HIG-13-003 and CMS-PAS-HIG-13-003.